UNIVERSITI
MALAYSIA
PERLIS

Annealing Effects on the Structural, Optical and Electrical Properties of Chemically Deposited CdS Thin Films using NH₄Cl Complexing Agent

[1]Rummana Matin, [1]M. S. Bashar*, [1]Munira Sultana, [2]Aninda Nafis Ahmed and [2]A. Gafur.

[1]Institute of Fuel Research and Development (IFRD), Bangladesh Council of Scientific and Industrial Research (BCSIR), Dhaka, Bangladesh.
[2]Pilot Plant and Process Development Center (PP&PDC), Bangladesh Council of Scientific and Industrial Research (BCSIR), Dhaka, Bangladesh.

ABSTRACT

This study aims to deposit different thicknesses of CdS thin films with a variation of deposition time by using chemical bath deposition technique. The aqueous solution of cadmium chloride, ammonium chloride, ammonium hydroxide and thiourea were used During the deposition process. The analysis was done to observe the effect of annealing on structural, optical and electrical properties of the CdS thin films. From the x-ray diffraction, this helps to confirm the cubic CdS phase formation, with a preferred orientation along (111). The finding indicates that the crystallite size is larger in films when it is deposited with low deposition rate. The crystallite size increased with increasing thickness and decreased after annealing. After annealing, the mobility and carrier concentration of the CdS thin films of different thicknesses is increasing and the resistivity decreasing. This study showed that the crystal structure, band gap, Urbach energy and electrical properties of CdS thin films can be changed when Cds thin films experienced annealing.

Keywords: Cds Thin Film, Chemical Bath Deposition, Annealing Effect, XRD, Band Gap.

1. INTRODUCTION

As a buffer layer in a solar cell, heterostructure cadmium sulfide (CdS) plays a significant role because of its properties as direct n-type semiconductor with a band gap of about 2.4 eV and large absorption coefficient of 4×10^4 cm^{-1} [1]. Among various other promising cadmium-free buffer layer; indium (III) sulfide (In_2S_3), Zinc sulfide (ZnS), tin sulfide (SnS), tin oxide (SnO), etc, CdS showed highest efficiency to be used in solar cells [2]. Among nonvacuum or sol-gel techniques; spray pyrolysis, spin coating, and dip coating, the chemical bath deposition (CBD) is known as most simple and low-cost method and produces uniform, adherent and reproducible films. In addition, the CBD technique is a low temperature technique and can be used for CdS deposition into a wide range of substrates.

Generally, the formation of CdS thin films by CBD is governed by two mechanisms, heterogeneous growth, i.e. ion by ion condensation of Cd^{+2} and S^{-2} ions on the substrate and homogeneous growth i.e. adsorption of colloidal particles on the substrate. At the earlier stage of deposition, the Cd^{+2} ions in the solution will form complexes with a complexing agent and NH_3. At this stage, more free Cd^{+2} ions are available in the solution and these ions react with S^{-2} ions and produce a cluster type of CdS particles. Thereafter when the concentration of Cd^{+2}

*Corresponding Author: bashar@agni.com

ions gradually decreases at higher NH_3 concentration, Cd^{+2} ions are strongly complexed by NH_3 ions. Due to this, there is no free Cd^{+2} ions are formed in the solution so that further formation of CdS particles is not possible. At this stage heterogeneous mechanism governs the deposition of a uniform thin layer of CdS [3, 4].

Previous studies focus on obtaining high quality CdS thin films by manipulating the parameters of CBD method, such as deposition time, temperature, pH value and by varying the concentrations of various reagents as well as their complexing agents [4–9]. The homogeneity and growth rate of CdS thin films depends on the use of complexing agent during chemical bath deposition. It is reported that good quality CdS thin films can be grown by using ammonia and ammonium chloride as the complexing agent [5]. The anions from the cadmium and ammonium salts are claimed to play a significant role when growing the CdS films. This role is suspected to be that of a complementary complexing agent [10,11].

There are several post deposition treatments such as annealing in N_2/Air/H_2 atmosphere at different temperatures have been carried out to see their effect on structural and optical properties of CdS thin film. Maticiuc *et al.* [12] found that different properties of CdS film are depending on the neutral, reducing or oxidizing annealing gas. Oxygen in phases $CdSO_3$ and CdO are observed from XRD patterns for air- and N_2- annealed CdS films at 400ºC. Longest N_2 annealing generated pure CdS layers, similarly with the H_2- annealed ones. Lichimura *et al.* [13] annealed CdS thin films at temperatures up to 500°C. The cubic phase of the as-deposited film remains dominant until the annealing temperature reach higher than 400°C. When the annealing achieves 450°C, the XRD pattern turns to that of hexagonal phase. The band gap is decreased by annealing done below 400°C and then abruptly increased by the annealing at 450°C. Islam *et al.* [5] annealed the CBD processed CdS thin films for 30 min at 400ºC and 500ºC, respectively in a vacuum furnace with pressure 500 mTorr. The cryatallinity of the films increased with increasing annealing temperature.

In this study, the low-cost CBD technique is used for the deposition of CdS thin films. Ammonia and ammonium chloride are used as the complexing agent. The CdS thin films are grown at different deposition time to analyze the film growth. The as-deposited films were annealed in N_2 environment at 430 ºC to see the annealing effect. The results found from the above analysis are compared for as-prepared and annealed CdS thin films of different thicknesses with respect to the preparation processes.

2. EXPERIMENTAL DETAILS

The CBD processed CdS thin films were grown onto sodalime glass substrates from the decomposition of thiourea in an alkaline solution containing a cadmium salt and suitable complexing agent ammonia (NH_3) and ammonium chloride (NH_4Cl). When $CdCl_2$ is used as Cd source, NH_4Cl is implemented as a buffer that controls the emission of ions during the deposition process. The combination helps to obtaina stable complex.

The substrates were cleaned successively using ultrasonic bath and degreased in methanol-acetone-methanol-deionized (DI) water for 10 minutes. Following to this, the degreased substrates is dried on a hotplate. CdS precursors were prepared with 0.0199 M of $CdCl_2$, 0.019835 M of NH_4Cl and 0.1423 M of Thiourea in DI water for all types of CdS thin films. First, a beaker containing DI water was immersed in the Chemical bath. The procedure continues by adding $CdCl_2$ with DI water and while continuously stirring, the NH_4Cl was added drop by drop into the mixture. The cleaned substrates were immersed in the beakers vertically; the beakers were then covered and heated. At 50 ºC ammonia was mixed with the solution. The Thiourea was mixed with the solution at the temperature of 80 ºC. The bath temperature was fixed at 80 ºC during deposition because, it has been deduced that, at low solution temperature conditions
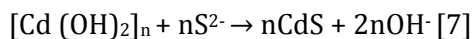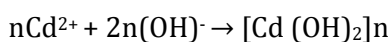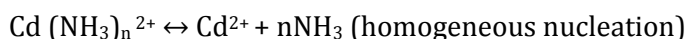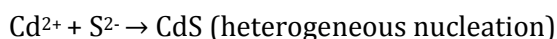
(Ts < 60 ºC), the deposition mechanism can be achieved only with a lower activation temperature process i.e. the ion by ion one. Whereas at higher temperatures (Ts > 60ºC), the deposition rate encompasses of larger activation energy, which lead the cluster by cluster process as the dominant growth mechanism. An increase in the solution temperature induces higher hydroxide cluster $Cd(OH)_2$ and sulfide ion concentrations [6]. In order to ensure that the pH is remained at 10, ammonia solution (28% of NH_3 solution) was then added to the solution. After the deposition process, samples were washed and ultrasonicated with DI water for 1 min to remove the surface impurities, and then dried on a hot plate. The deposition time was varied from 20, 30 and 40 minutes to obtain different thicknesses. The deposited thin films were annealed in an annealing chamber (MTI corporation, GSL– 1100X) in N_2 environment under a dynamic vacuum of around 2 Torr and at 430ºC temperature for 1 hour.

The Surface Profilometer (DAKTAK-150) is used to measure the thickness of the cadmium sulfide (CdS) thin films. Later, the X-ray diffraction analysis (XRD) was performed, by a Bruker D8 XRD with copper kα radiation to investigate the crystalline structure of the materials. The absorbance and transmittance were recorded using a duel beam UV-vis spectrophotometer (Shimadzu, UV-1601V). This spectrometer was used to measure the relative transmittance and absorbance of CdS thin films. The sheet resistance was measured by a four-point probe measurement set-up and the mobility and carrier concentration was measured by a Hall effect measurement setup (ECOPIA, HMS-3000, SK).

3. RESULTS AND DISCUSSIONS

3.1 Deposition Rate

Figure 1 shows the change in thickness of CdS thin films with increasing deposition time. It is observed that the thickness increases faster following slower increase with increasing deposition time. It has been reported that heterogeneous process is highly desirable rather than homogeneous deposition for uniform thin films. Adding to that, the homogeneous process forms precipitation of CdS in the solution resulting non-adherent powdery films. The reactions for both processes are given as follows:

$Cd^{2+} + S^{2-} \rightarrow CdS$ (heterogeneous nucleation)

$Cd (NH_3)_n{}^{2+} \leftrightarrow Cd^{2+} + nNH_3$ (homogeneous nucleation)

$nCd^{2+} + 2n(OH)^- \rightarrow [Cd (OH)_2]n$

$[Cd (OH)_2]_n + nS^{2-} \rightarrow nCdS + 2nOH^-$ [7]

In our case, the precipitation of CdS is observed after 30 minutes of deposition. This is because at the earlier stage of deposition, the CdS films are dominantly governed by the heterogeneous mechanism and shows a uniform thin layer. However, this thin layer is gradually growing with the homogeneous mechanism. Ouachtari *et al.* reported that increasing the concentration of the cadmium ions in the CBD process produces a higher final film thickness; also, longer deposition time is needed to attain the final film thickness. In addition, after a certain deposition time, the absorption and/or dissolution process predominates over the heterogeneous and homogeneous precipitation [11].
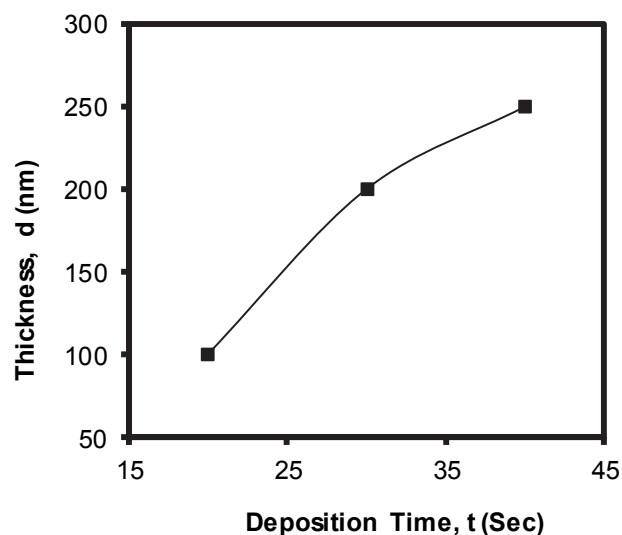
Figure 1. Variation of thickness at different deposition time.

3.2. Crystal Structure

It is reported that cadmium sulfide can exist in both sphalerite cubic and hexagonal forms. Cubic CdS grows in the zincblende structure by considering metastable phase [14]. The XRD patterns of CdS thin films are shown in Figure 2. Three diffraction peaks matched with JCPDS 01-074-9663 correspond to (111), (220) and (311) reflections at 2Θ of 26.5°, 44°, and 52°, respectively indicating that the obtained CdS films have a cubic structure with the preferential orientation normal to the (111) direction. A similar film structure has been reported previously by other researchers [15, 16]. All the XRD patterns exhibit a broad hump near the (002) peak at $2\theta = 26.7°$, which is due to the glass substrate. A comparison between the spectra of the films shows that the peak intensity increases when the deposition time is increasing i.e. with increasing thickness the thicker film has more crystallinity than the thinner films. The degree of preferred orientation along (111) increased when the thickness is increases. The peak intensity of each of the three films increased after annealing indicating an increase in crystallinity [16]. Annealing helps the atoms to rearrange themselves and eliminate defect density in the film resulting in good crystallinity. Tomas *et al*. [17] reported that the N_2 or Ar annealing brings reorientation of as-deposited CdS films with a significant improved crystalline quality by increasing the grain size and decreasing the number of grain boundaries in CdS films. Also, such some annealing leads to phase transition from the metastable cubic phase to a stable hexagonal phase of CdS [18], which is undesirable when stacking CdS film with a cubic CdTe absorber [12]. In our case CdS, thin films are not gone through any phase transition but improved in structural orientation due to annealing at 430°C in the N_2 environment.

The crystalline size of the CdS thin films film is calculated using FWHM data and Debye-Scherer formula [13].

$$d = \frac{\lambda}{\beta \cos \theta_B} \tag{1}$$

where d is the calculated grain size of the film, λ is the wavelength of x-ray radiation (1.54059Å of CuKα radiation). β is full width at half-maximum (FWHM), θ_B is a peak position of the diffracted X-ray beam. The particle sizes calculated are 5.62, 2.38 and 1.53nm for as-deposited and 4.7, 1.53 and 1.38nm for annealed CdS thin films deposited for 20, 30 and 40 mins

respectively. Thus, it can be concluded that the particle size increased when the thickness is increased and decreased after annealing.

Moulkia *et al*. (2009) [6] explained the reduction of the grain size by the variation of the growth rate. At high deposition rates (thicker films), the nucleation step is fast, therefore the nucleation sites concentration is large. Due to this, the nuclei size enlargement is limited and blocked by the surrounding nuclei. However, at low deposition rates (thinner films), the low concentration of the nuclei sites enables the nuclei to grow and attain a larger size. Consequently, the grain size is larger in films deposited with low deposition rate.
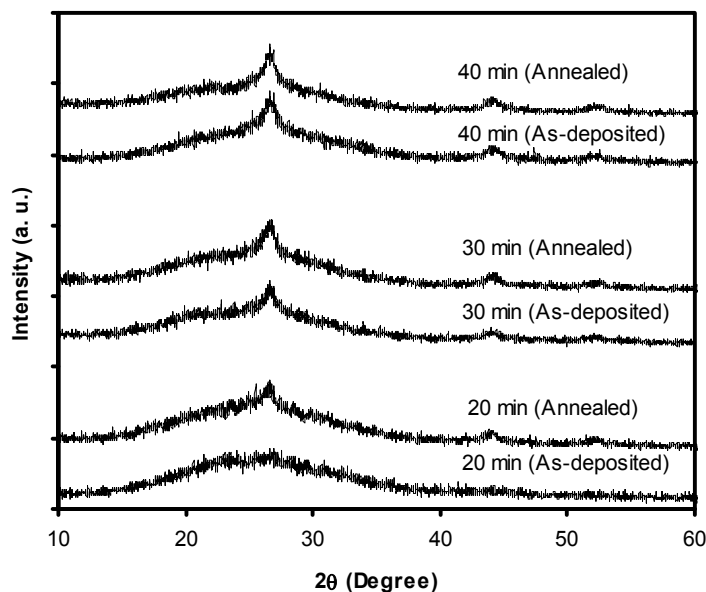

Figure 2. Superimposed XRD pattern of as-deposited and annealed CdS thin films deposited for 20, 30 and 40 minutes.

3.3. Optical Properties

UV-Vis spectrometry is used to observe the optical properties such as transmission, absorption and optical band gap of the thin films. A blank sodalime glass slide was placed in the beam direction during the scanning process. Figure 3(a) and 3(b) shows the variation of transmittance T (%) with wavelength λ (nm) in the wavelength range from 300 to 800nm for as-deposited CdS thin films of various deposition time and 20 min deposited annealed CdS thin film. The maximum transmittance observed are 82%, 58%, and 84% respectively in the visible region (400 to 700 nm). Figure 3(b) shows that the transmittance T (%) is decreasing after annealing due to the denser CdS formation during the process [5]. It is found that the annealed CdS thin films exhibit the maximum transmittance (between 40% to 75%) in the visible range and have sharp fall at the band edge which is good for optoelectronic devices, especially for solar cell window layers, confirming the presence of crystallinity of CdS thin films [5, 21].
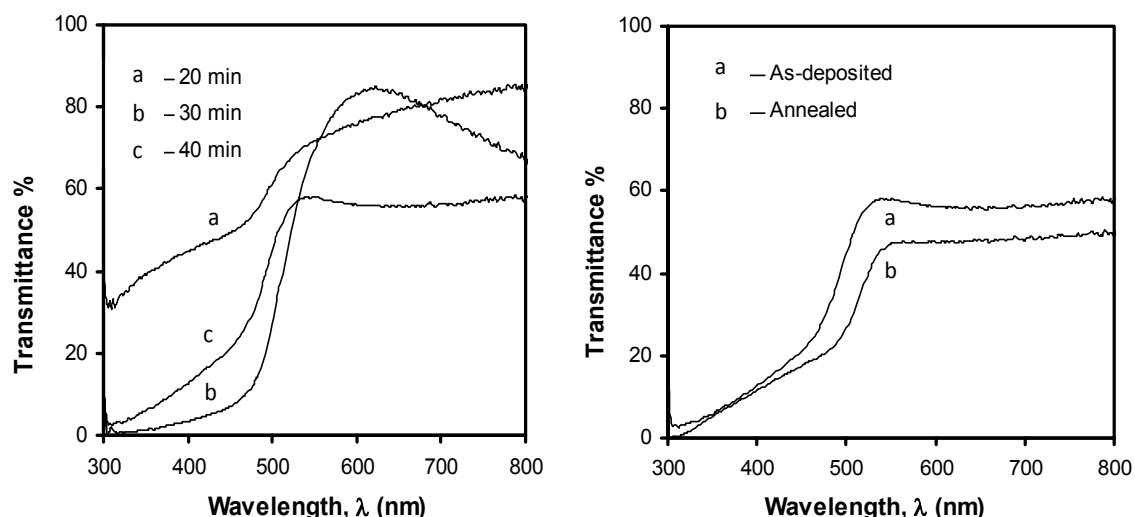
Figure 3. Transmittance vs. wavelength plots for (a) Different deposition time (b) As-deposited and annealed CdS thin films.

Figure 4(a) shows the variation of absorbance measured in the wavelength ranging from 300 to 800nm with the variation of deposition time i.e. 20, 30 and 40 min. Due to the variation of deposition time the thicknesses were found about 100, 200 and 250nm for 20, 30 and 40 min respectively. Figure 4(a) shows an increase in the absorbance when the CdS film thickness is increasing. Figure 4(b) represent an increase of absorbance after annealing which indicates the formation of denser CdS thin films due to annealing. The finding is similar to the study from Islam *et al.* [5]. From the absorbance spectra, it is also observed that for all types of CdS thin films the maximum absorbance of CdS thin films is observed at around 300nm. In the visible region the absorbance rises very rapidly before 300 nm, attains its maximum value and then decreases rapidly up to 600nm i.e. the absorbance decreases rapidly from ultraviolet to visible region.
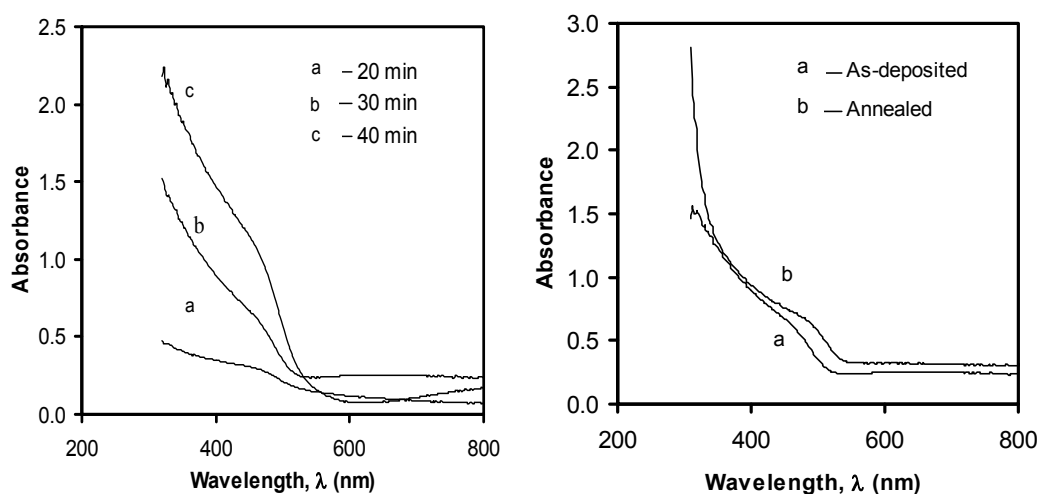

Figure 4. Absorbance vs. wavelength plots for (a) Different deposition time (b) As-deposited and annealed CdS thin films.

The absorption coefficient, α, [22] is calculated from the measured absorbance data for different wavelengths corresponding to different photon energies at room temperature using equation (2).

$$\alpha = 2.303\frac{A}{d}$$

(2)

where $A = \log_0(\frac{I_0}{I})$ is the absorbance and d is the thickness of the film. An idea of the band structure and electronic transition involved in absorption process can be obtained by studying the dependence of optical absorption coefficient on the photon energy.

The spectral dependence of α, on the photon energy, hν, for as-deposited and annealed CdS thin films is shown in Figure 5. The absorption coefficient of all CdS thin films increases with increase in photon energy. The absorption co-efficient increased due to annealing indicating denser films.
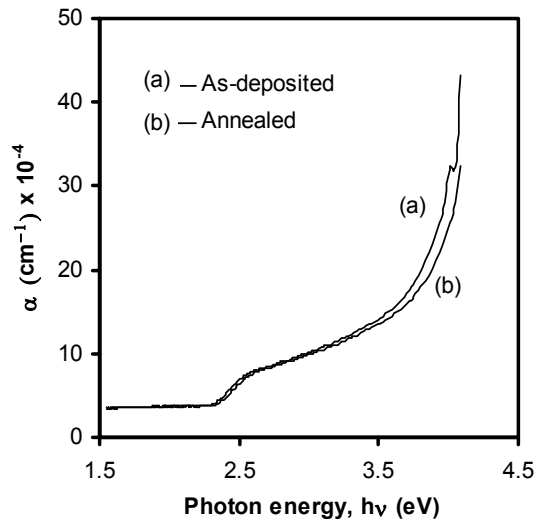

Figure 5. Absorption coefficient vs. photon energy plots for as-deposited and annealed CdS thin films.

In crystalline and amorphous materials, the photon absorption is observed to obey the Tauc relation [23],

$$\alpha h\nu = B (h\nu - E_{opt})^n$$

(3)

where, hυ is the incident photon energy, h Planck constant, ν the frequency of incident radiation, B an energy independent constant, E_{opt} the optical band gap and n is an index depending on the type of optical transition caused by photon absorption. The index n equals ½ and 2 for accepted direct and indirect transitions respectively. Therefore, the direct transition energy gap (E_{qd}) can be obtained by plotting $(\alpha h\upsilon)^2$ versus hν curve and then extrapolating the linear portion of the plots to the intercept in the hν axis. Figure 6 shows the change in band gap due to annealing. An increase in the band gap of CdS thin films is observed after annealing. The band gaps obtained for as-deposited and annealed CdS thin films of different thicknesses are listed in Table 1. From Table 1 it can be depicted that the band gap energy is changing from 2.66 to 2.82 eV for as-deposited CdS thin films of different thicknesses and for annealed that are ranged from 3.60 to 3.87 eV for CdS thin films of different thicknesses. The increase of band gap after annealing can be attributed due to the formation of CdO during annealing. It is observed that the band gap changes slightly with the variation of deposition time i.e. there is a little increase of band gap with increasing thickness may be due to some structural changes as

also depicted from XRD. But after annealing the band gap decreased with increasing thickness. This may be due to the fact that, as the thickness is increasing, the relative amount of formation of CdO decreases. This happens because the CdO forms onto the surface of the CdS. But when the thickness increases, the O_2 cannot penetrate the thicker films. On the other hand, it is found that the band gap energy of the CdS thin films increased significantly after annealing. This occurrence can be explained based on the O_2 incorporation. Similar explanation on annealed CdS thin film has previously reported by Islam (2013) [5]. Wu *et al.* (2004) studied on RF-sputtered CdS deposition using an O_2/Ar atmosphere and showed that the CdS:O films become transparent in the wavelength range above the band gap of CdS and suggested that CdS films grown with inclusion of oxygen during deposition can be a better choice for thin film solar cells as oxygenation will further increase their band gap [21]. The changes of band gap with increasing annealing temperature are caused by changes in the defects, the composition and the crystalline properties of the CdS thin films. The spectral dependence of α was studied at photon energies less than the band gap of the films.
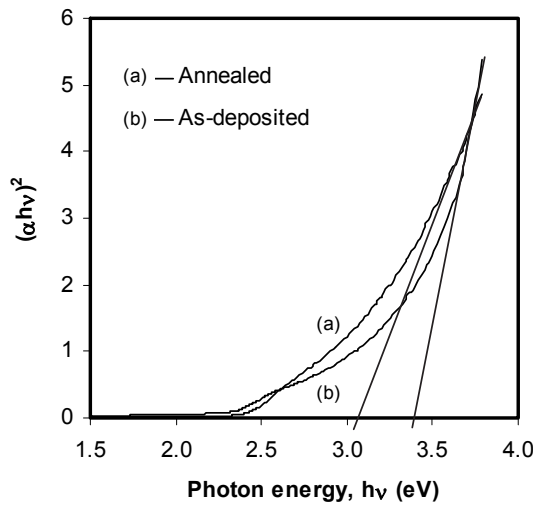

Figure 6. $(\alpha h\nu)^2$ vs. $h\nu$ plots for as-deposited and annealed CdS thin films.

The Urbach energy is calculated from the slope of the plots of $\ln\alpha$ vs $h\nu$. This slope gives the width of the localized states associated with amorphous states in the band gap at photon energies less than the band gap. The absorption coefficient near the fundamental absorption edge is exponentially dependent on the incident photon energy [24].

$$\alpha = \alpha_0 \exp (h\nu/E_u) \tag{4}$$

where α_0 is a constant and E_u is the Urbach energy. Thus, the plots of $\ln\alpha$ should be linear whose slope gives Urbach energy. The $\ln\alpha$ vs $h\nu$ plots for as-deposited CdS thin films of different thicknesses are shown in Figure 7(a) and that of annealed CdS thin films are shown in Figure 7(b). The Urbach energies are calculated from the slopes of the Urbach plots and are listed in Table 1. The Urbach energies are ranging from 2.61 to 5.1 eV for as-deposited and 2.34 to 3.4 eV for annealed CdS thin films of different thicknesses. From Table 1 that as the thickness increased the band gap and tail width of CdS films increased due to the increase in disorder/ impurity and film stoichiometry with thickness or deposition time. Dingyu *et al.* [20] reported that the change of band gap and tail width are related to film stoichiometry in which it changes with deposition of the parameter. It can be noticed that the Urbach energy decreases after annealing for all the thicknesses. This behavior may be due to a decrease in the degree of disorder and decrease in density of defect states (which results in the reduction of tailing of bands). Due to this, it showed an increase in crystallinity. It is also found that the Urbach

energy increases with increasing thickness indicating an increase in disorder or defects with thickness or deposition time.
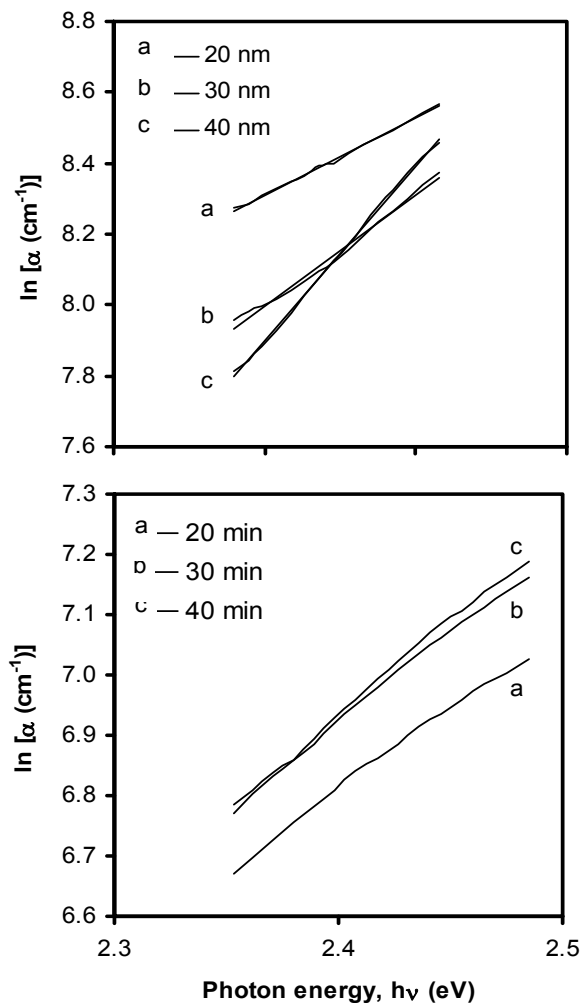

Figure 7. Urbach plots (lnα vs hν curves) for (a) as-deposited CdS thin films with different thicknesses and (b) annealed CdS thin films with different thickness.

Table 1 Variation of band gap with the deposition time of as-deposited and annealed CdS thin films

CdS thin film	Deposition Time (min)	Film Thickness (nm)	Band Gap (eV)	Urbach energy (eV)
As-deposited	20	100	2.66	2.61
	30	200	2.75	3.60
	40	250	2.82	5.10
Annealed	20	100	3.87	2.34
	30	200	3.70	3.12
	40	250	3.60	3.40

3.4. Electrical Properties

To characterize the electrical properties of the thin films, Four Point probe and Hall effect measurements are performed in air at room temperature. The as-deposited films exhibit semiconducting behaviors with resistivity in the range of $10^{-2}\Omega$.cm for as-deposited CdS thin films and $10^{-3}\Omega$.cm for annealed CdS thin films. The resistivity decreased one order of magnitude after annealing. This decrease is attributed to the improved crystallinity, growth in grain size and the improvement in film stoichiometry, as is indicated by the XRD patterns. n-type conductivity is observed by the Hall measurements for both types of the CdS thin films. The mobility and carrier concentration of as-deposited and annealed CdS thin films are given in Table 2. It is observed that both of the mobility and carrier concentration of the CdS thin films of different thicknesses are increasing (and accordingly the resistivity decreases) after annealing. Generally, the carrier concentration and mobility have increased due to the interstitial Cd^{+2} ions or sulfur vacancies which exist in the film. These carriers act as donors and results in an increase in the carrier concentration as well as a consequent decrease in the resistivity [10]. Any significant change in carrier concentration and mobility is not observed due to thickness variation.

Table 2 Electrical parameters for as-deposited and annealed CdS thin films

CdS thin film	Film Thickness (nm)	Resistivity (Ohm.cm)	Mobility (cm^2/Vs)	Carrier concentration (cm^{-3})
As-deposited	100	4.08×10^{-2}	9.62×10^{1}	5.45×10^{11}
	200	5.00×10^{-2}	1.46×10^{0}	2.80×10^{11}
	250	6.43×10^{-2}	5.40×10^{1}	9.62×10^{11}
Annealed	100	3.32×10^{-3}	2.96×10^{1}	1.60×10^{12}
	200	2.21×10^{-3}	1.41×10^{2}	3.05×10^{12}
	250	1.81×10^{-3}	1.68×10^{2}	6.12×10^{12}

4. CONCLUSION

In this study, the investigation is carried out to explore the structural, optical and electrical properties of CBD deposited films. It is found that at the earlier stage of deposition, the CdS films are dominantly governed by the heterogeneous mechanism because it shows a uniform thin layer. However, gradually the CdS films finished with homogeneous growth. Apart from this, from the XRD pattern, the graph indicated showed that the peak intensity increased when the deposition time is increasing. Also, the peak intensity of each of the three films increased after annealing indicating an increase in crystallinity. The optical band gap lies in the range of 2.66 to 2.82 eV for as-deposited and 3.6 to 3.87 eV for annealed CdS thin films of different thicknesses. The Urbach energies are ranging from 2.34 to 5.1 eV for as-deposited and 2.61 to 3.4 eV for annealed CdS thin films of different thicknesses. Both of the mobility and carrier concentration of the CdS thin films of different thicknesses increase (and accordingly the resistivity decrease) after annealing. The structural, optical and electrical properties of CdS thin films are improved after annealing. These CdS thin films deposited by CBD technique, with the added advantages of cost-effective, large area deposition and easy thickness control, can be very important for solar cell application.

REFERENCES

[1]   L. B. Freund, S. Suresh, Thin film materials stress, defect formation and surface evolution, Cambridge University Press, UK (2003).

[2]   Y. Sánchez, M. Espíndola-Rodríguez, H. Xie, S. López-Marino, M. Neuschitzer, S. Giraldo, M. Dimitrievska, M. Placidi, V. Izquierdo-Roca, F. A. Pulgarín-Agudelo, O. Vigil-Galán, E. Saucedo, Solar Energy Materials & Solar Cells **158** (2016) 138.

[3]   J. M. Doňa, J. Herrero, J. Electrochem. Soc. **144** (1997) 4081.

[4]   C. K. Kumar, N. T. Q. Hoa, S. G. Yoon, E. T. Kim, Journal of the Korean Physical Society **55** (2009) 284.

[5]   M. A. Islam, M. S. Hossain, M. M. Aliyu, P. Chelvanathan, Q. Huda, M. Karim R. K. Sopian, N. Amin, Energy Procedia **33** (2013) 203.

 [6]   H. Moualkia, S. Hariech, M. S. Aida, N. Attaf, E. L. Laifa, J. Phys. D: Appl. Phys. **42** (2009) 135404.

[7]   R. K. Choubey, D. Desai, S. N. Kale, S. Kumar, J Mater Sci: Mater. Electron. **27** (2016) 7890.

[8]   R. Y. Mohammed, S. Abduol, A. M. Mousa, International Letters of Chemistry, Physics and Astronomy **11** (2014) 146.

[9]   K. Lingeswaran, S. S. P. Karamcheti, M. Gopikrishnan, G. Ramu, Middle-East Journal of Scientific Research **20** (2014) 812.

[10]   H. Khallaf, I. O. Oladeji, G. Chai, L. Chow, Thin Solid Films **516** (2008) 7306.

[11]   F. Ouachtari, A. Rmili, S. E. B. Elidrissi, A. Bouaoud, H. Erguig, P. Elies, J. Mod. Phys. **2** (2011) 1073.

[12]   Natalia Maticiuc, Mart Kukk, Nicolae Spalatu, Tamara Potlog, Malle Krunks, Vello Valdna, Jaan Hiie, Comparative study of CdS films annealed in neutral, oxidizing and reducing atmospheres, Energy Procedia **44** (2014) 77.

[13]   Masaya Ichimura, Fumitaka Goto, Eisuke Arai, Structural and optical characterization of CdS films grown by photochemical deposition.

[14]   J. N. Ximello-Quiebras, G. Contreras-Puente, G. Rueda-Morales, O. Vigil, G. Santana-Rodrı´guez, A. Morales-Acevedo, Solar Energy Materials & Solar Cells **90** (2006) 727.

[15]   F. Lisco, P. M. Kaminski, A. Abbas, K.Bass, J. W. Bowers, G. Claudio, M. Losurdo, J. M. Walls, Thin Solid Films **582** (2015) 323.

[16]   HMetin, R Esen, Annealing effects on optical and crystallographic properties of CBD grown CdS films, Semicond. Sci. Technol. **18** (2003) 647.

[17]   Tomas SA, Vigil O, Alvarado-Gil JJ, Lozada-Morales R, Zelaya-Angel O, Vargas H, Ferreira da Silva A, Influence of thermal annealings in different atmospheres on the band-gap shift and resistivity of CdS thin films. J Appl Phys **78**(4) (1995) 2204.

[18]   Mishra S, Ingale A, Roy UN, Gupta A. Study of annealing-induced changes in CdS thin films using X-ray diffraction and Raman spectroscopy. Thin Solid Films **516** (2007) 91.

[19]   Ed. F. A. Devillanova, W. W. D. Mont, Hand Book of Chalcogen Chemistry, The royal society of chemistry, UK (2013).

[20]   Yang Dingyu, Zhu Xinghua, Wei Zhaorong, Yang Weiqing, Li Lezhong, Yang Jun, and Gao Xiuying, Structural and optical properties of polycrystalline CdS thin films deposited by electron beam evaporation, Journal of Semiconductors 32 (2011).

[21]   X. Wu, Y. Yan, R. G. Dhere, Physics Status Solidi C **4** (2004) 1062.

[22]   M. Birkholz, Thin Film Analysis by X-ray Scattering Wiley-VCH, Frankfurt, Germany (2006).

[23]   J. Tauc, A. Menth, D. Wood, Phys. Rev. Lett. **25** (1970) 749.

[24]   F. Urbach Phys. Rev. **92** (1953) 1324.